UNIVERSITY OF CALIFORNIA,
IRVINE

Novel Electrocardiogram Monitoring Devices Using Non-Contact Electrodes

THESIS

submitted in partial satisfaction of the requirements
for the degree of

MASTER OF Science

in Electrical and Electronics Engineering

by

Zhijie Zhang

Thesis Committee:
Assistant Professor Hung Cao, Chair
Professor Nikil Dutt
Assistant Professor Zhou Li

2021

DEDICATION

To

my parents and friends

in recognition of their worth

A feeling bears on itself the scars of its birth; it recollects as a subjective
emotion its struggle for existence.
it retains the impress of what might have been, but is not.

(Alfred North Whitehead
Process and Reality)

and hope this world come back from Covid-19

If the fool would persist in his folly he would become wise.

William Blake
Proverbs of Hell

TABLE OF CONTENTS

LIST OF FIGURES

LIST OF TABLES

ACKNOWLEDGEMENTS

I would like to express the deepest appreciation to my committee chair, Professor Hung Cao, who has the real love for science and engineering. He continually and convincingly conveyed a spirit of adventure in regard to research and scholarship, and an excitement in regard to teaching. He is not only a professor but also a friend to me. Without his guidance and help, it's not possible for me to graduate.

Secondly, I would like to thank my teammate, Tai, who is a very kind and generous PhD student in our lab and joined our lab two years earlier than I did. We knew each other in the spring of 2019, and he introduced me to join Hero Lab at the beginning. My work is based on what he had already. We worked together in the past one year. I learned a lot from him. And it's also very lucky for me to have a friend like Tai during Covid-19.

Thirdly, I would like to thank my committee members, Professor Zhou Li and Professor Nikil Dutt, who are very enthusiastic and passionate to their work and to students. Their help means a lot to me.

This project is approved by IRB #2020-6342.

ABSTRACT OF THE THESIS

Novel Electrocardiogram Monitoring Devices Using Non-Contact Electrodes

by

Zhijie Zhang

Master of Science

in Electrical and Electronics Engineering

University of California, Irvine, 2021

Professor Hung Cao Irvine, Chair

Among electrophysiological indices, cardiac signal in the form of electrocardiogram (ECG) has been the most popular and widely used signal, not only for patients but also for healthy populations for vital sign or well-being monitoring. However, during the COVID-19 pandemic with practice of social distancing, hospital visits are not recommended and convenient. The recent advances in electronics, Internet of Things (IoT) and data sciences have paved the way for continuous electrophysiological monitoring for humans in the home setting. However, for a special group of population like pregnant women, weekly visits are still required during the third trimester of pregnancy. This calls for a home-based portable and comfortable device which could be used to monitor both the mother and the fetus. In this thesis, we develop a flexible sensor patch that can fit the anatomical surface of people's abdomen which can measure ECG signals continuously and wirelessly. Instead of using traditional contact electrodes, we investigate the potential of non-contact electrodes which could be unobtrusive and more comfortable. The abdominal ECG signals are transferred to an Android smart phone via Bluetooth Low Energy (BLE) communication. To monitor the

mother and the fetus, in-house schemes have been developed to extract fetal ECG and maternal ECG. We characterized the non-contact electrodes using impedance analysis and tested with different insulation materials and thicknesses. We then validated the patch in different cases like sitting, standing and walking, mimicking practice scenarios. We also further validated the entire system with pregnant women.

INTRODUCTION

With the development of IOT, continuous biomedical monitoring for human body is comparatively applicable in recently years. And among all of the biomedical monitoring parameters, ECG is significantly important compared with other parameters. Combined with ECG signal and certain signals, scientists or doctors are able to explore and note much more information which is hidden before. For example, they can calculate their heart beats per minute with the support of ECG as the practically simplest application. In addition, the blood pressure can be calculated with the application of ECG signal and PPG signal [1]. Moreover, fetal ECG seems to be the most promising way to detect fetal hypoxia [2] [3] [4]. especially during Covid-19.There would be lower risk of infection if pregnant women are able to do EEG tests at home instead of going to hospital And what's the importance is the detection and analysis of biological electrical signals from the surface of the skin is non-invasive and more convenient compared with other methods like ultra-sound. In addition, this method has significant persuasiveness if people would like to apply it for long-run tests.

For almost the past 70 years, the mainstream clinical application of bio-potential acquisition systems, wet resistive electrodes applied directly to the surface of the skin, has not been changed [5]. This technology has certain drawbacks such as limiting the system practical deployment into the effective, casual and consumer driven, non-research-oriented markets. Firstly, wet electrodes are difficult, inconvenient and time-consuming due to the requirement of electrolytic gel. It can also be painful as it is often necessary to use an abrasive process to remove grease and particles from the skin prior to electrode placement to achieve an ideal test environment and desired low impedances [6]. What's more, the gel can also

diffuse through the subject's hair causing nearby sensors and result in limiting the effective spatial resolution. Besides, the gel will eventually dry out during the tests and alters the impedances. Hence re-application is necessary for this traditional method [7].

Then, about 40 years ago, dry resistive electrodes came up and became popular [8]. Dry electrodes do not require electrolytic gel as they incorporate impedance transforming electronics next to the measurement site (the skin-electrode interface). Due to this reason ,tt's more convenient for people to use . However, without the wet interface, these electrodes are more susceptible to skin irregularities like sweat, grease and hair as well as motion artifacts. In addition, dry electrodes also suffer from the necessity for constant uniform electrical contact. As the result, any displacement away from the surface of the skin or friction against the skin could cause significant disruptive artifacts [9] [10].

However, even though attractive advantages mentioned above that dry electrodes have, this method still need to be placed with skin directly. In order to solve that the issue, researchers thought about using capacitive electrodes (non-contact electrodes), which is a kind of more recent technology of dry electrodes. By insulating the detection disc of the sensor, the electrode-skin interface is considered in the same way as a parallel plate capacitor [11]. As with dry resistive electrodes, capacitive electrodes are highly sensitive to artifacts caused by movement and environmental noise [12].

At the same time, due to the weak coupling of the electrode to the skin under measurement, high signal attenuation is observed in non-contact capacitive electrodes compared to traditional wet electrodes. Some special techniques such as neutralization and guarding also require an increasing number of components or larger area in the electrode

circuit [13]. All mentioned factors increase the size of detection disk to approximately double the diameter of typical wet electrodes (from 9–12 mm to 25 mm) [14] [15].

However, despite these issues, capacitive electrodes have been considered with great potential and to be capable of acquiring bio-potentials signals that rival that of traditional electrode technologies [16] because some obvious reasons such as convenience and non – invasive feature. Even though it is challenging, the bright future is expected by professions as well as the public. Hence, in this thesis, it is focused on the characteristics of non-contact electrode itself, looking for the effect caused by different materials and different thickness.

What's more, non-invasive sensor is competitive for long-run, portable measurements. Considering about that, a sensor patch embedded in belts is designed and fabricated so people especially pregnant women can wear this sensor on their abdomen or anywhere they prefer in the future. The basic functionality of this sensor is validated by doing some characterization tests and real tests with pregnant volunteers.

Chapter 1

Hardware Part

1.1 Overview

This sensor patch is intended to use on abdomen which is soft and curvilinear. And our electrodes require a good contact with skin. Especially for non-contact electrodes, good contact between skin and insulation layer as well as insulation layer between electrodes is necessary. Due to this reason, our board must have flexibility. Flex-rigid design is used here. Fig 1.1 shows how the patch looks like. The whole size for this board is 95 mm by 135 mm. The size of our main board is 95 mm by 45 mm. The distance between the centers of corresponding electrodes is 10 cm. And because we will use wet electrode as a standard to

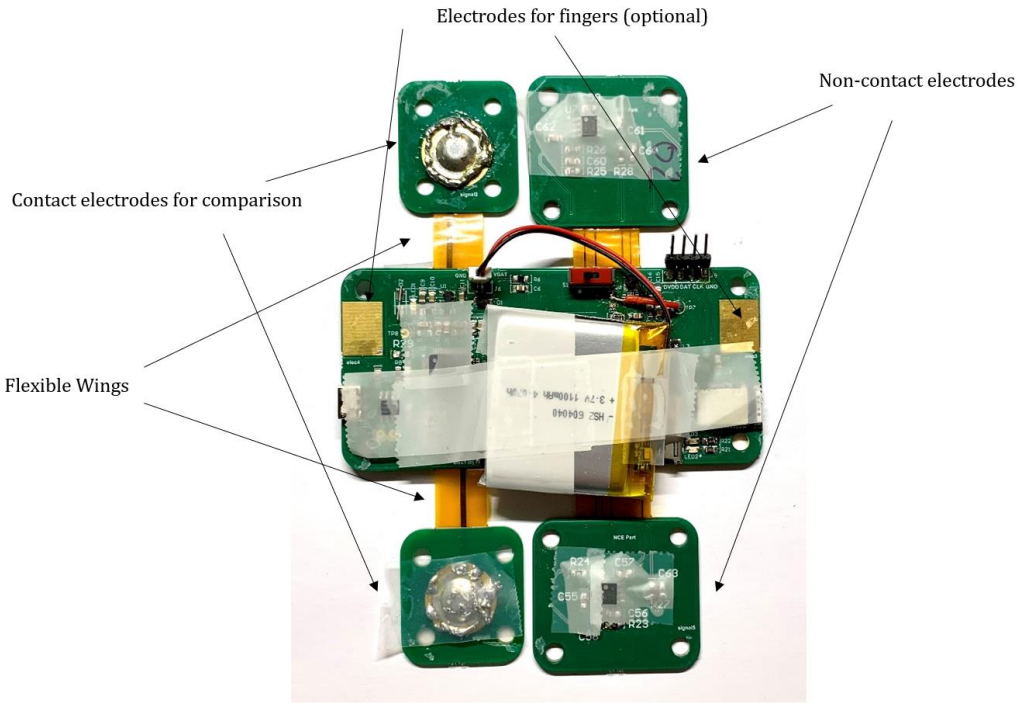

Fig 1.1 Picture of the whole device

validate non-contact electrodes later, we put the wet electrode and non-contact electrode as close as possible. We create a four-layer PCB and pour copper at every layer to provide protection of our signals and insulation from noise. And another reason is that four-layer is the minimum number to support a flex-rigid design.

We can see the flexible part clearly in Fig 1.1. This wireless device use Bluetooth to communicate with a smart phone and use a 3.7V lithium battery as its power. I have 3 channels of signal and each channel contains 2 electrodes. Channel 1 is the wet contact electrode which we use as our gold standard. Channel 2 is the copper pad electrode on the top layer of this PCB board which provide optional and additional ECG signals from fingers. Channel 3 is what I want to validate and test. I will provide details about this one in the corresponding part. These electrodes will measure signal in different cases and for different aims.

1.2 Overview of Electrocardiogram

Electrocardiogram is a kind of voltage signal of how the electrical activity of the heart changes with time as action potentials propagate throughout the heart during each cardiac cycle which is basically a consequence of cardiac muscle depolarization followed by repolarization [17]. An ECG signal conveys a great amount of information to a trained doctor. ECG can be used to measure the rate of heartbeats, the size and position of heart chambers and the potential of any disease about heart or conduction system [18].

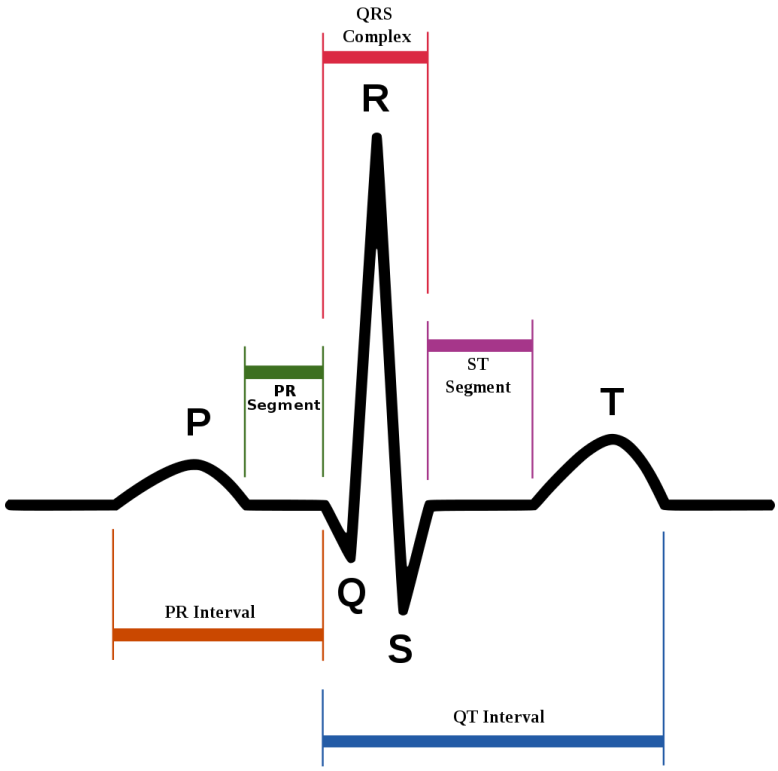

Fig 1.2 Schematic ECG diagram of normal sinus rhythm for a human heartbeat.

Here is a normal ECG plot including three main components, P wave, QRS complex and T wave. P wave which is characterized by 5 – 30 Hz frequencies represents the depolarization of the atria. QRS complex which usually contains within 8-50 Hz frequencies represents the depolarization of the ventricles. Some higher frequencies (above 70 Hz) of QRS wave also convey information about abnormal ventricular conduction. As well as T wave which lays mostly within a range from zero to 10 Hz represents the repolarization of the ventricles [19] [20]. QRS frequencies at the 24-80 Hz range have been found as the most informative part in a recent study. And importantly, most of commercially available ECG devices routinely provide ECG signal with a frequency range up to 150 Hz [20].

Basically, there are four diverse forms of noise: baseline wander, 60 Hz power line interference, muscle noise and motion artifact [21].

1.3 Board Circuit Components

There are 5 main parts in this whole design including ADS Part, BLE Module, Power Supply, Battery Circuit and NCE Part.

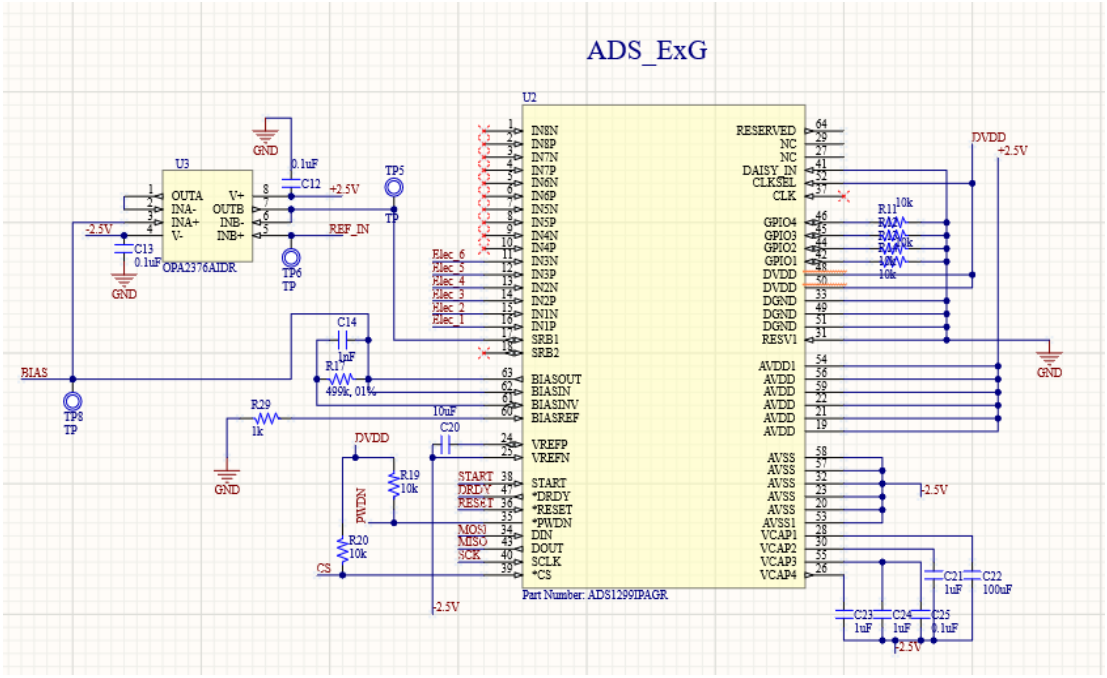

Fig 1.3 The schematic close-up of ADS 1299 circuit

Fig 1.3 is the schematic for the ADC Amplifier. ADC is very important because the performance of ADC decides the quality of the signal. Here I use ADS 1299 which is an 8-channel, 24-bit ADC. This chip is designed for biomedical signal measurement which has built-in right leg drive amplifier (BIAS pin) and built-in oscillator and reference what will be very helpful when people design a biomedical measurement system. The gain of this ADC is also programmable. In the mode I choose (gain = 12), the input-referred noise is 2.9 μV_{pp}.

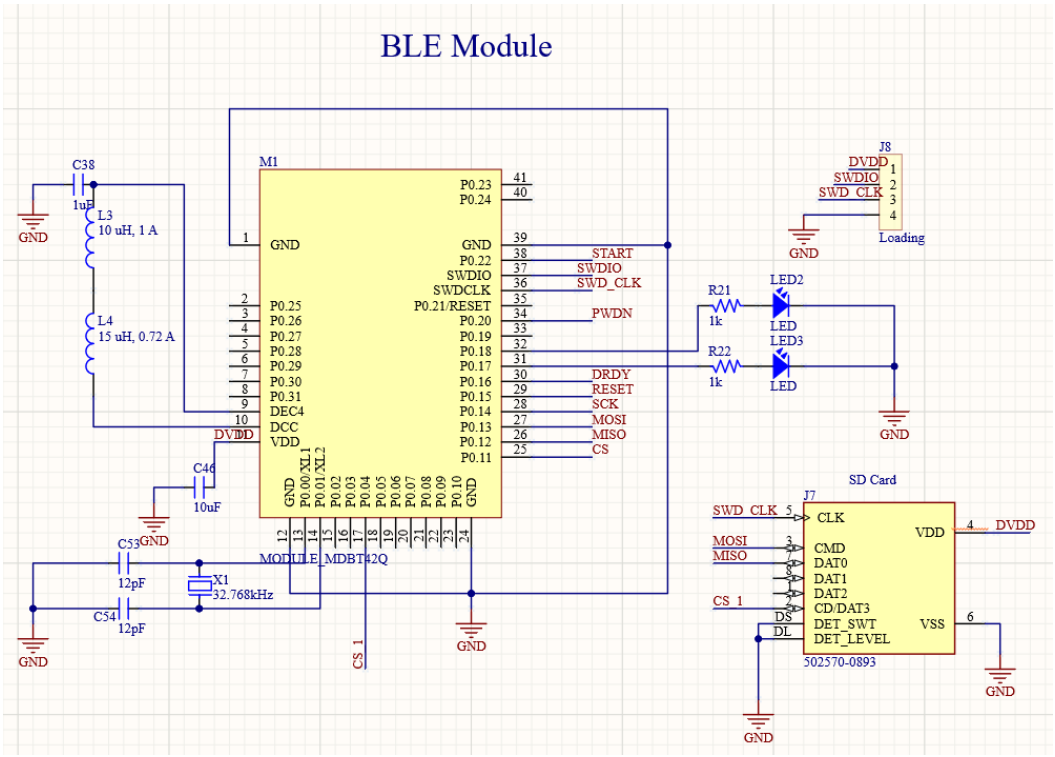

Fig 1.4 The schematic close-up of Bluetooth module and SD card pocket

Fig 1.4 is the schematic of Bluetooth module. I use nRF 52832 from Nordic Semiconductor as the main micro controller which is a general-purpose multiprotocol SoC which has lots of features like Bluetooth low energy, protocol concurrency and generous memory availability for both Flash and Ram. And with an Arm Cortex-M4 CPU with floating point unit running at 64 MHz, it has a great potential to control many circuit components and do calculation on chip. But due to the board was made in our lab by hands, and the pins of nRF 52832 are too close to solder them, I chose a package of nRF 52832 called MDBT 42Q which contains a nRF 52832 inside but with larger pin distance.

The Bluetooth module use a Serial Wire Debug (SWD) protocol to communicate with a PC. SWD uses an ARM CPU standard bi-directional wire protocol and is defined in the ARM Debug Interface v5. The basic function requires 4 pins, SWDIO, which is the data transfer

interface, SWD_CLK which provides the clock for both pc and microcontroller, DVDD and GND.

In order to make our sensor patch more portable, I add a SD card pocket at bottom right corner of Fig 1.4 so this system can run individually and store the data into a SD card instead of connecting to a smart phone all the time.

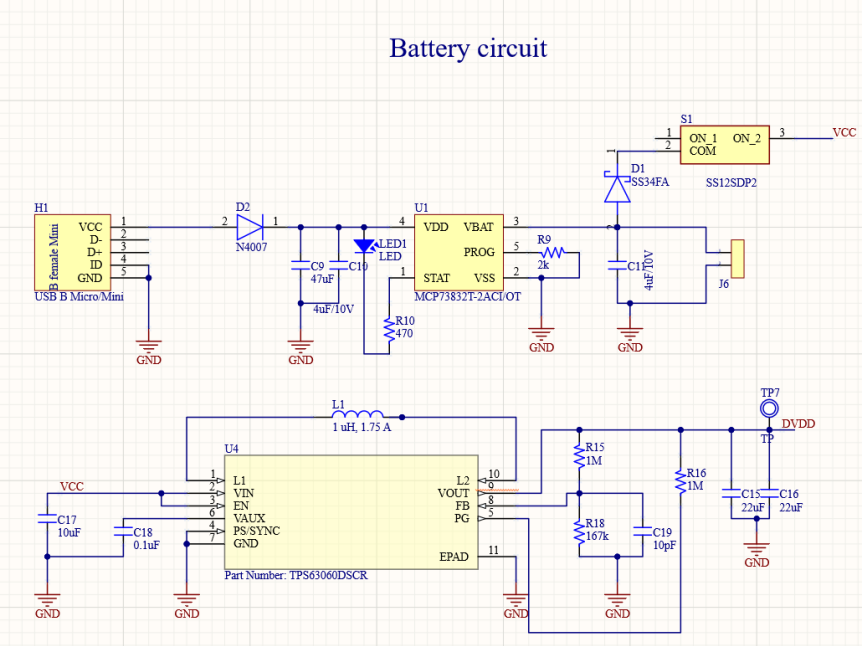

Fig 1.5 The schematic close-up of battery circuit part

Because our Bluetooth module requires a very strict power voltage. And a stable power voltage of amplifier and ADC is also necessary to have a good signal. So, we apply a buck/boost circuit between the battery and our real circuit loads.

$$R15 = R18 \times \left(\frac{V_{out}}{V_{FB}} - 1\right) \tag{1.1}$$

V_{out} and V_{FB} are the voltage of the corresponding pin in Fig 1.5. The typical current into the FB pin is 0.01 μA. And the voltage across the resistor between FB and GND (V_{FB}) is typically 500 mV. It is easy to calculate V_{out} based on R15 and R18 or choose the value of these two resistors based on V_{out}. This circuit can provide a stable 3.5V power voltage.

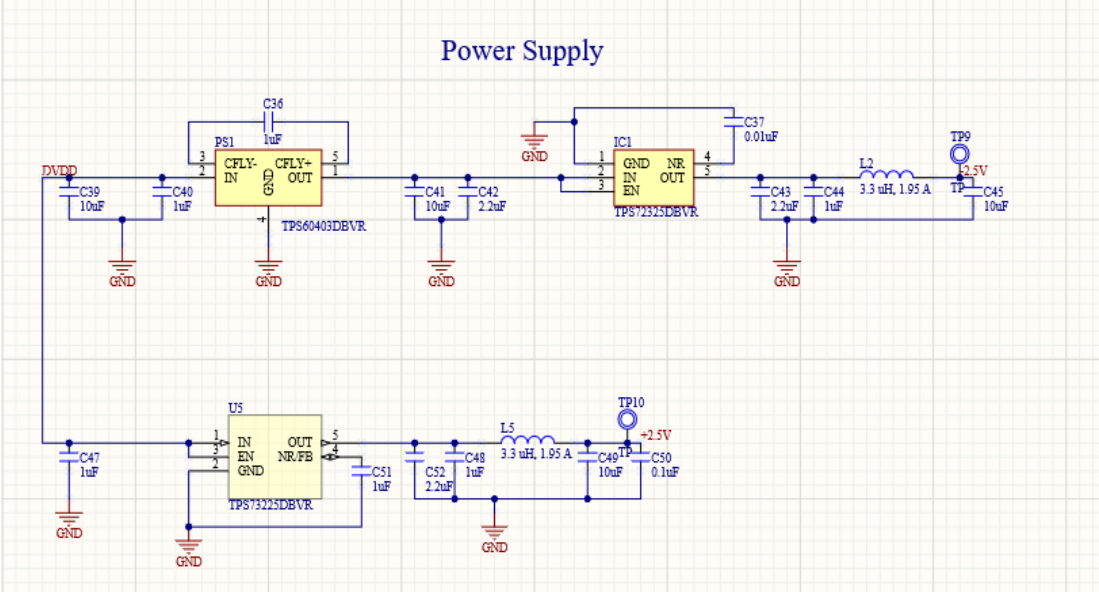

Fig 1.6 The schematic close-up of power supply part

Due to there are several voltage level we will use in our circuit such as 3.5 V, 2.5 V and - 2.5V required by ADS 1299, we need an additional voltage switch circuit to transfer our power supply voltage from 3.5 V to 2.5 V and – 2.5 V. And these power supply should be stable to support ADS 1299 to get good signals.

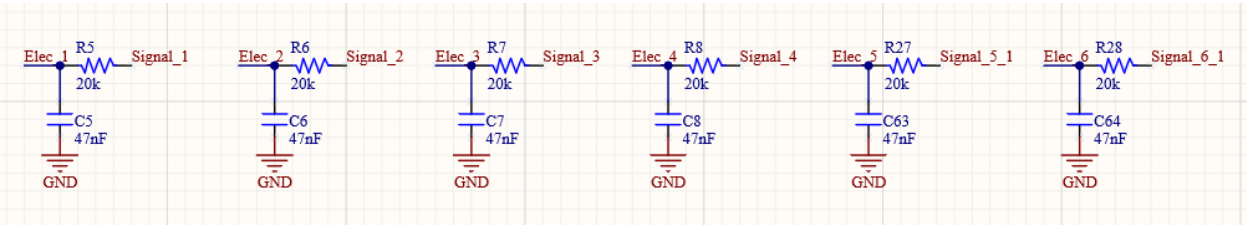

Fig 1.7 Lowpass filter part

As for the noise cancelling part, we use both hardware method and software method to reduce noise. In hardware part, I apply a lowpass RC filter between each sensor pad and ADS 1299 amplifier.

Fig 1.8 High-pass filter and low-pass filter

In Fig 1.6, the left one is a high-pass filter and the right one is a low-pass filter. For RC filter, we can use this equation to calculate the cut-off frequency (where the attenuation is 3 dB) or choose the value of components in the opposite.

$$f = 1/2\pi RC \tag{1.2}$$

The cut-off frequency of low-pass filter in Fig 1.5 is 169.4 Hz which covers the most important ECG frequency range of 0 – 150 Hz.

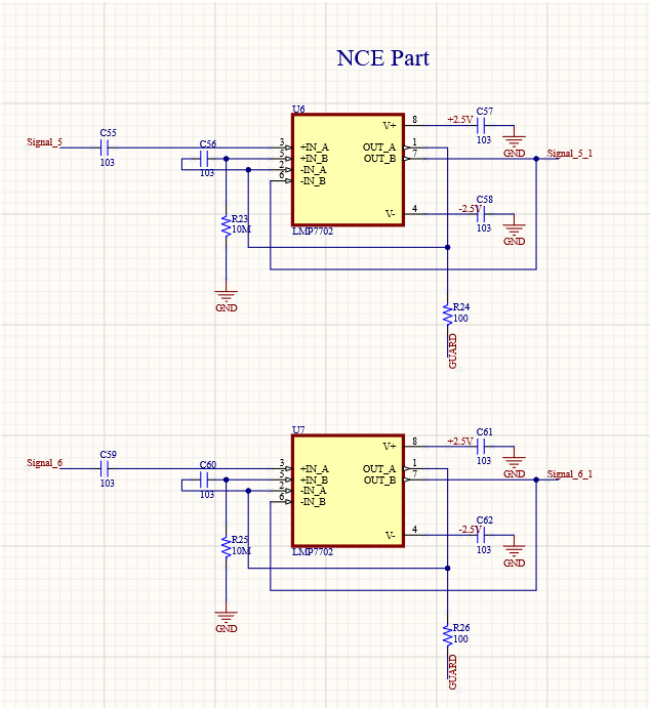

Fig 1.9 Non-contact electrodes part

The Non-contact electrodes are the most important part in this circuit. We want to validate this kind of sensor in abdominal ECG field and discover the characterization of non-contact electrodes. This part will be explained in Chapter 2.

1.4 SPI Connection

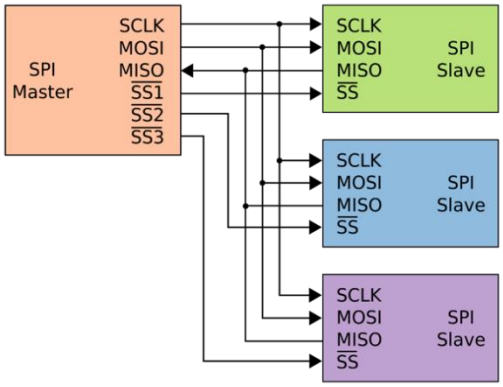

Fig 1.10 Typical SPI bus: master and independent slaves

The Bluetooth module MDBT 42Q is the microprocessor, the 'brain', in this circuit. The chip communicates with ADS 1299 and SD card pocket via SPI protocol. SPI means serial peripheral interface, which is a synchronous serial communication interface specification used for short-distance communication, especially in embedded systems. This protocol contains two kinds of devices, master device and slave device. SPI is one master and multi slave communication. The SPI bus specifies four logic signals:

- SCLK: Serial Clock (Output from master)
- MOSI: Master Out Slave In (data output from master)
- MISO: Master In Slave Out (data output from slave)
- SS: Slave Select (often active low, output from master)

Because we have two independent slave components in our circuit, an ADS1294 ADC and a SD card socket. Fig 1.3 shows how we should connect our master device, the Bluetooth module, and the two slave components together.

Chapter 2

Non-Contact Active Electrode

2.1 Model for Skin-Electrode Interface

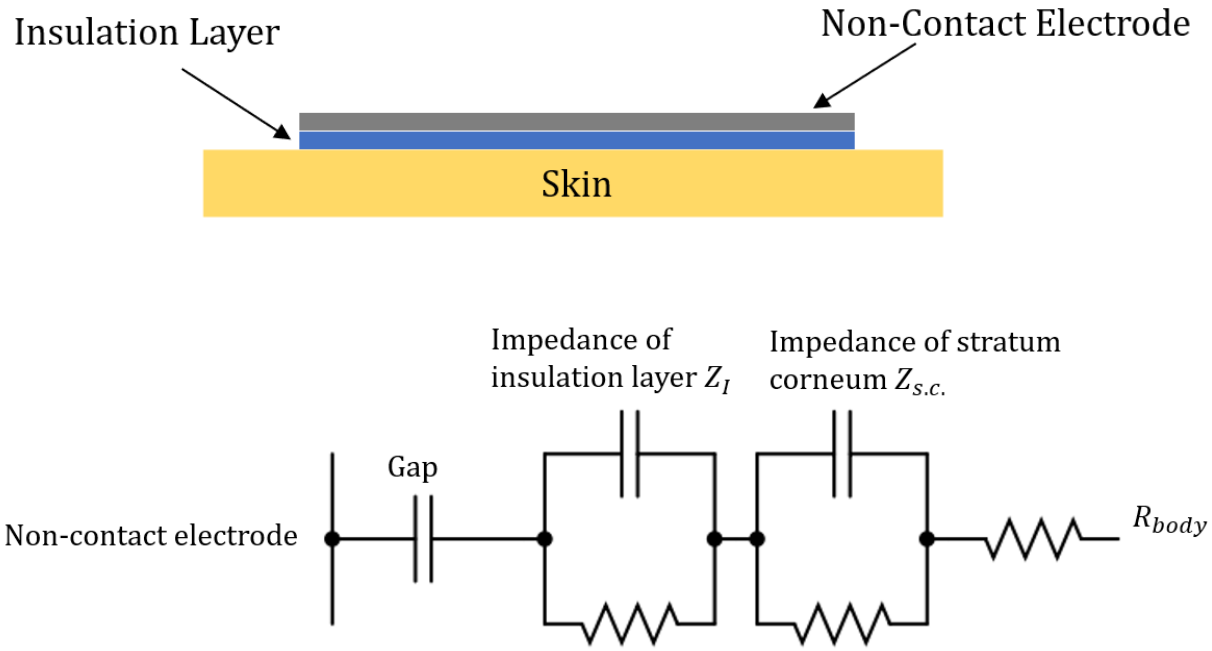

Fig 2.1 Simplified topology and electric model of non-contact active electrode

This is a simplified topology and electric model of non-contact electrodes. In general, the coupling between electrodes and skin can be described as a layered capacitive and conductive structure as shown in Fig 2.1. The system impedance mainly contains the capacitance of the gap C_g, the impedance of insulation layerZ_I, the impedance of stratum corneum $Z_{S.C.}$ and the resistance of human body R_{body}. For each series of parallel RC elements, typically one of RC components will dominate the other and the coupling could be represented as a single element with conductance g_C in parallel with capacitance C_C. If we let $Y_C(j\omega)$ represent the coupling admittance [22]. We will get

$$Y_C(j\omega) = g_C + j\omega C_C \quad (1.3)$$

Typically, the value of C_g is at the range from 1 pF – 1 nF with good contact. But in practice, this value may keep changing due to body and electrode movement. Depending on the kind of insulation materials, the impedance of insulation layer has a wide range. That's also we want to test in this thesis. The total system impedance may go up to 100 mega ohms or even higher.

2.2 Non-contact Active Electrode Design

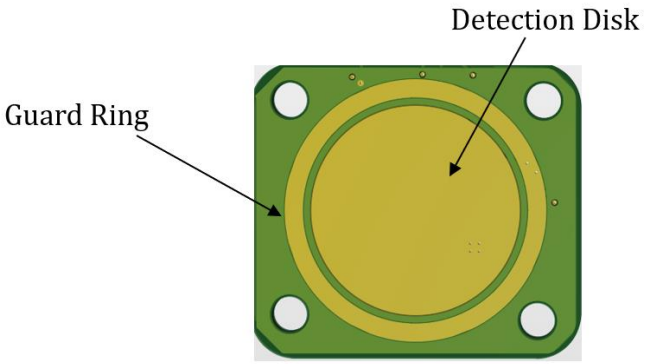

Fig 2.2 Close up of non-contact electrode

The non-contact electrode includes 2 parts, detection disk and guard ring. The diameter of the detection disk is 25 mm. This pad is made of copper and printed directly to the PCB bottom layer and connected with top layer through several vias.

Because of the high impedance skin-electrode interface, this electrode is very sensitive to environmental noise. Therefore, it is beneficial to create a guard ring surrounding the detection disk, constructing a complete Faraday cage. It's also helpful to remove parasitic capacitance effects such as capacitive signal division. There is a 1 mm gap between detection disk and guard ring [7].

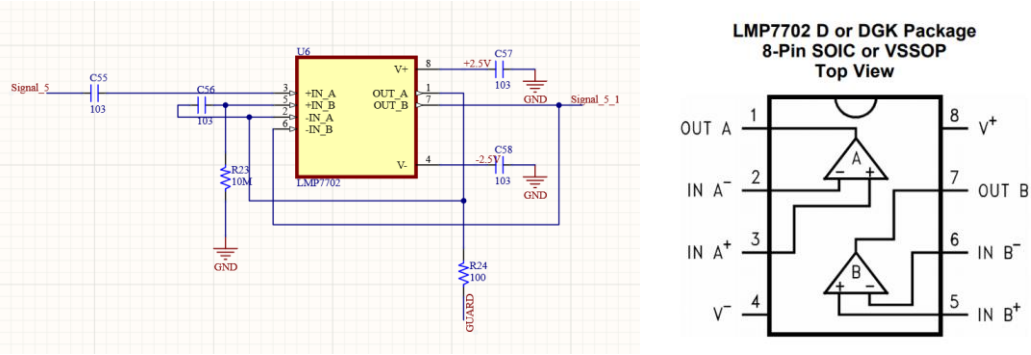

Fig 2.3 The schematic of NCE circuit and the schematic of LMP 7702

Based on LMP 7702 from TI (Texas Instruments), we build a very simple active non-contact electrode with high quality.

The LMP7702 is a dual low-offset voltage, rail-to-rail input and output precision operational amplifier. It can work with an ultra-high impedance but a much lower supply voltage. As Fig 2.3 above shows, we use both amplifiers inside in our circuits. We can call them 7702-A and 7702-B separately.

7702-A is configured as a unity-gain voltage buffer. The 10 nF (C55) and 100 Ω (R24) resistors are used to protect the input of the amplifier. They can also provide isolation from the output of the amplifier from the active shield. We don't have an external input bias here. And because 7702 has rail-to-rail input/output range and is configured as unity gain, inputs and outputs keep stable. This method is better than adding a bias network here. Because definitely we can't say a non-contact electrode works in a good environment. It's hard to do denoising and decoupling work with non-contact electrodes. A bias will add a lot of noise. However, the lack of bias also brings a DC operating point/ drift and we can't know the exact value of it. In order to solve this problem, we use a passive RC high pass filter with a cut-off frequency of 1.6 Hz to remove the drift as well as low frequency noise. V_{guard} is a reference voltage here. Then second opamp 7702-B buffers this high-passed signal and drives the cable

connecting the electrode to the main board for post data transferring and processing. Having a unity gain buffer also eliminates the need for impractically precisely matched passive components at the electrode to achieve a good common-mode rejection ratio (CMRR) [22].

There is one thing we need to understand that 7702 here is used as two separate buffers instead of an amplifier. The signal (channel 3) will be sent to ADS 1299 for amplification and digitalization as the same case as signal of channel 1 and channel 2 which are signals from wet contact electrodes and copper electrodes on the top layer of PCB board. And that means all the 3 channels have the same gain, the gain of ADS 1294. We can analyze and compare them directly.

Another thing we need to know is that this configuration of circuit can't eliminate low frequency noise or drift 100%. We just choose a better way to avoid such noise which will be caused by adding a bias network. Noise caused by other factors is still there, especially the movement of human or electrode itself. Sometimes such noise will still dominate our signals.

Chapter 3

Experiments and Results

3.1 Experiments Setup

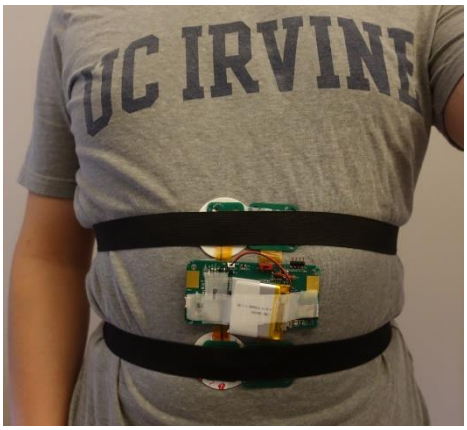

Fig 3.1 Experiment Setup

This project is under Hero Lab of UCI and under IRB #2020-6342.

Keeping a good and stable contact with skin or insulation layer is vital important when people measure ECG signals using non-contact electrodes. As Fig 3.1 shows, we use two flexible belts to fix our sensor board. And because we use a flex-rigid PCB design, our electrodes fit the curve of abdomen perfectly. In Fig 3.1, we can only get signal from non-contact electrodes and can't get the signal from wet electrodes because wet electrodes require a direct contact with skin. If we want to measure both signals, we need to take off clothes.

When we do real ECG test on volunteers, we will ask them to stand up first to wear the patch with the belts. Then they are suggested to sit down, keep standing or lie on the bed depending on the aim of that test to relax and put their hands on the board to provide a little more force which is helpful to keep a good and stable contact of skin-electrode interface. The

patch is put below belly button. We will tighten the belt after they become relaxed then start the measurement.

3.2 Bluetooth Communication

It's recommended that searching for some exist code packages and examples of Bluetooth chip first. As for nRF 52832, Nordic Semiconductor provides lots of detailed examples to guide you. In our case, the Bluetooth module sends data package to a smart phone every 40 ms. Each package contains 5 kinds of information including header codes, index of every time point and the data of 3 channels. Header codes are used to let the smart phone recognize this data package. Index number has a range from 0 to 255. At the end of every loop in our board, this number will add 1 automatically. This is used for checking our signal integrity. For example, if we see the index number jumps to 200 from 195 directly, it means we lose the data from index 196 to 199. Typically, the communication between smart phone and our board is not stable at the first 3 seconds. Then everything will be fine. The sampling rate is set to 500 Hz.

3.3 Android Application

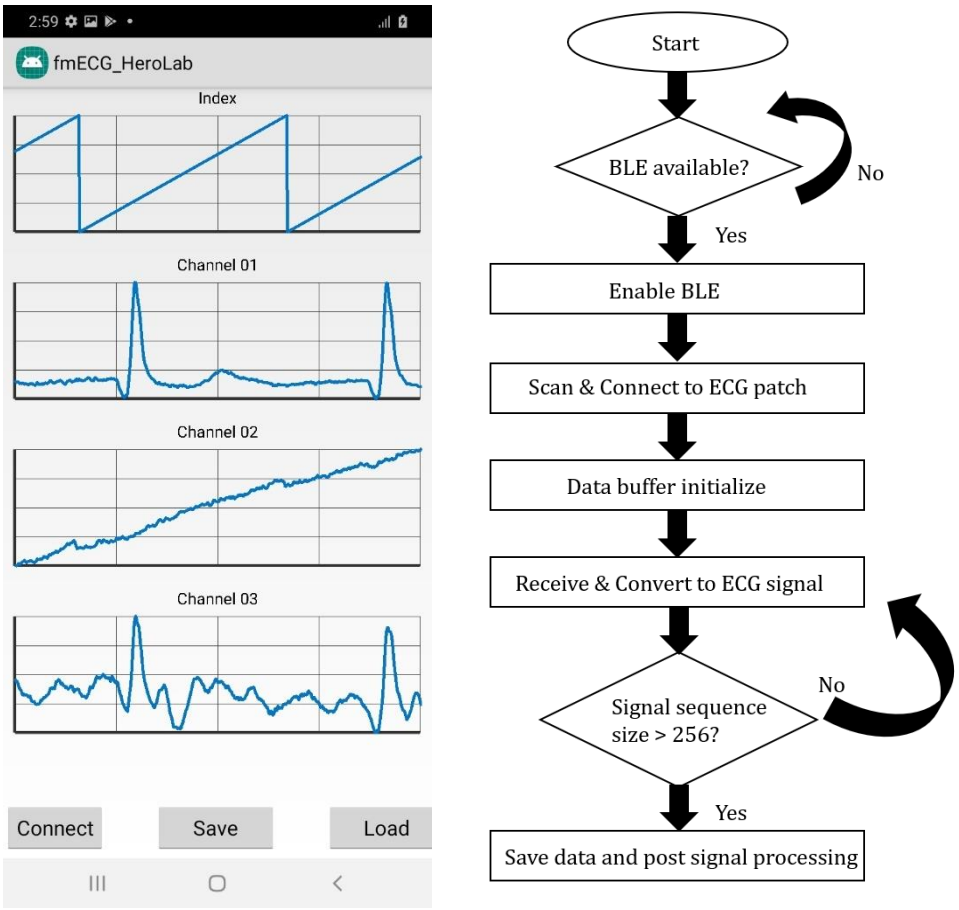

Fig 3.2 A screenshot of Android application and its operation flow chart

We developed an Android application for transferring and saving our signals. The meaning of Index and Channel 01 to 03 has been explained before.

Once the application is turned on, it will keep checking if the Bluetooth is available. We need to allow the Bluetooth function for this application and then scan all the Bluetooth devices and choose our patch from the list. The app starts to receive data after we click the device name of our patch. In each data package received via Bluetooth, the format of header codes is uint32 while the format of all the data is uint16. We need to convert uint16 to decimal number we can analyze directly [23]. Data will be saved in a buffer temporarily and then be saved into a text file once the size of buffer goes up to 256. At the same time,

the real-time signal will show up on the phone screen. We don't have any signal processing program in this Android application. All the data will be processed later in MATLAB.

3.4 Post Signal Processing

We use a 16-order notch filter of 60 Hz and an 8-order bandpass filter at a range of 0.1 Hz to 150 Hz to remove power line noise and other frequency components we don't want.

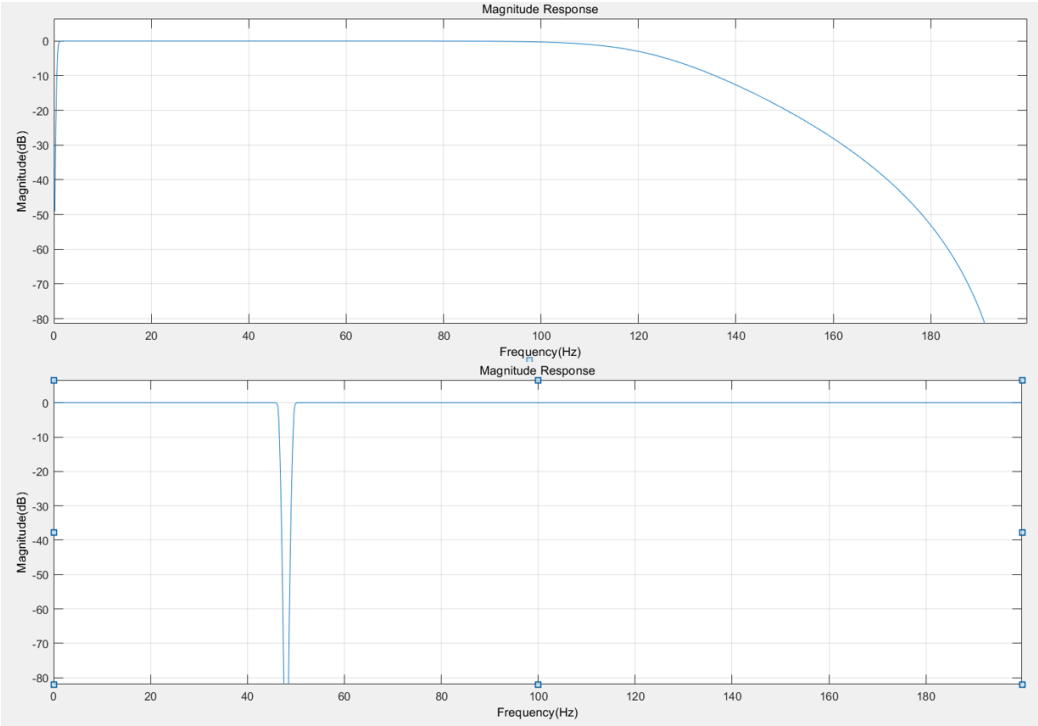

Fig 3.3 Frequency response of two filters

The first figure of Fig 3.3 is the frequency response of bandpass filter and the other one belongs to the frequency response of notch filter. Both filters use the Butterworth filter. The frequency response of the Butterworth filter is maximally flat in the passband, in which case we can get uniform gain, and rolls off towards zero in the stopband. Compared to the Chebyshev filter or the Elliptic filter, the Butterworth filter rolls off more slowly around the cutoff frequency but without ripple.

3.5 Wet ECG

AgCl wet electrodes are our gold standard here. The gel, the belts and our flex-rigid design make the electrodes have a very good contact with skin. Fig 3.4 shows some measurement results of sitting, standing and walking. We can see the quality of signals is very good in every scenario.

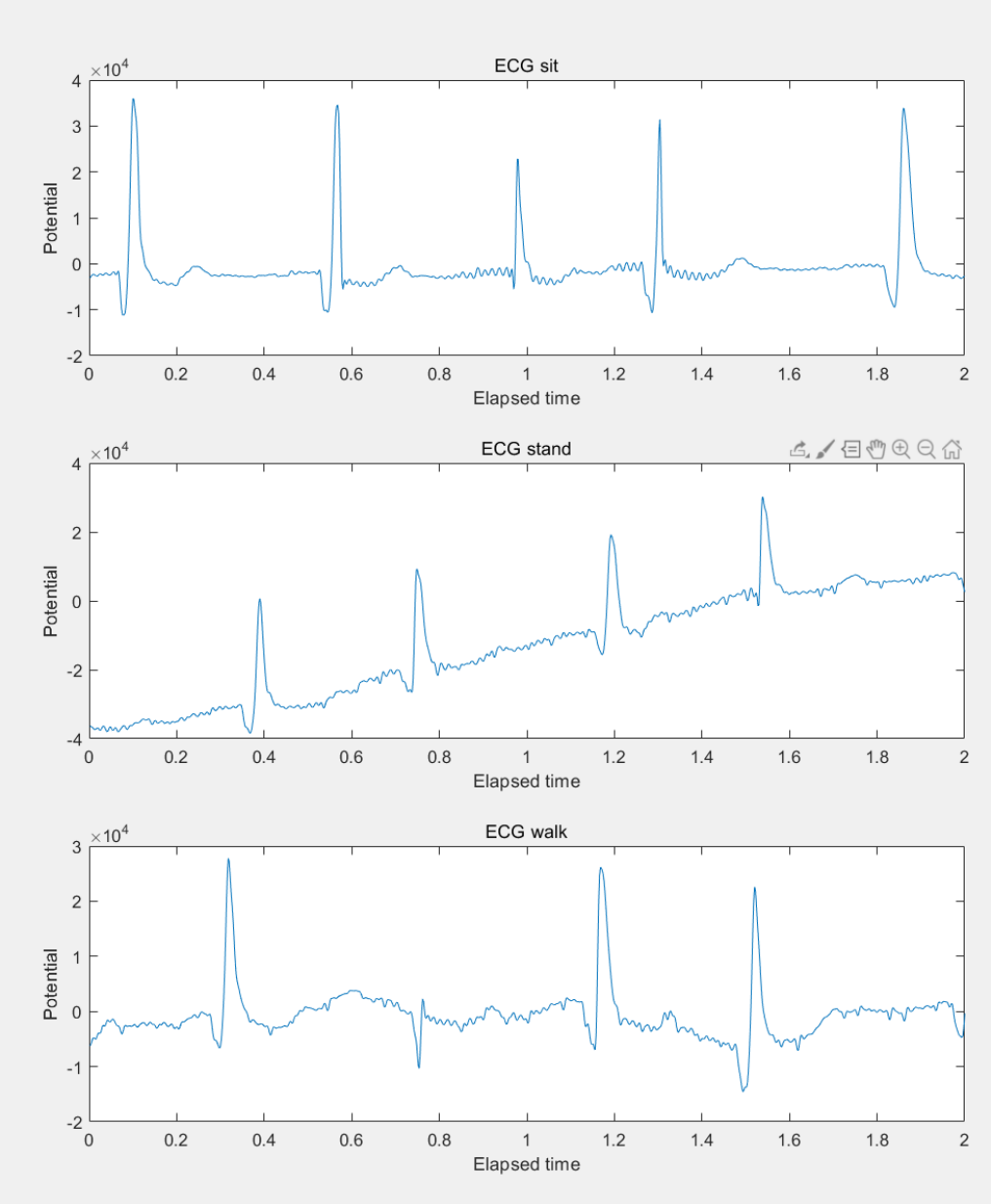

Fig 3.4 ECG signal of AgCl electrodes under sit, stand and walk scenario

These are very good signals. But we can still see the signal get a little bit worse when we change from sitting to standing, or walking. That's the influence of the contact between electrodes and skin. Intense action will cause bad contact.

3.6 Non-contact Electrode

3.6.1 Impedance of Different Materials

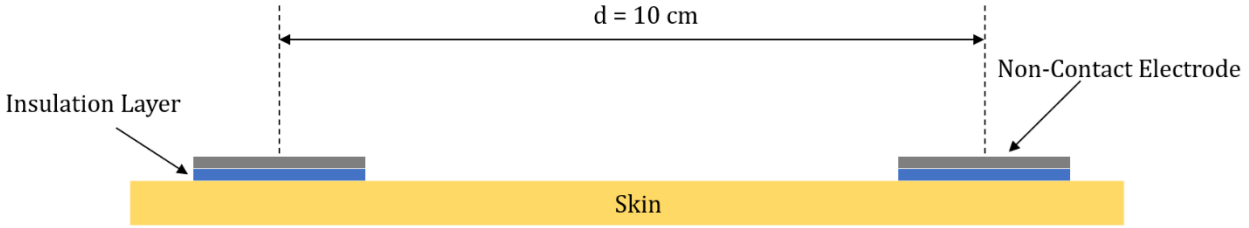

Fig 3.5 Principle impedance measurement setup

Here is a simple topology about the impedance test of non-contact electrodes. We use CHI 760E potentiostat from CH Instrument to test the impedance of non-contact electrodes. When doing such tests, we disconnect the electrode with other components to make sure there is not any interference from other circuit components and circuit itself.

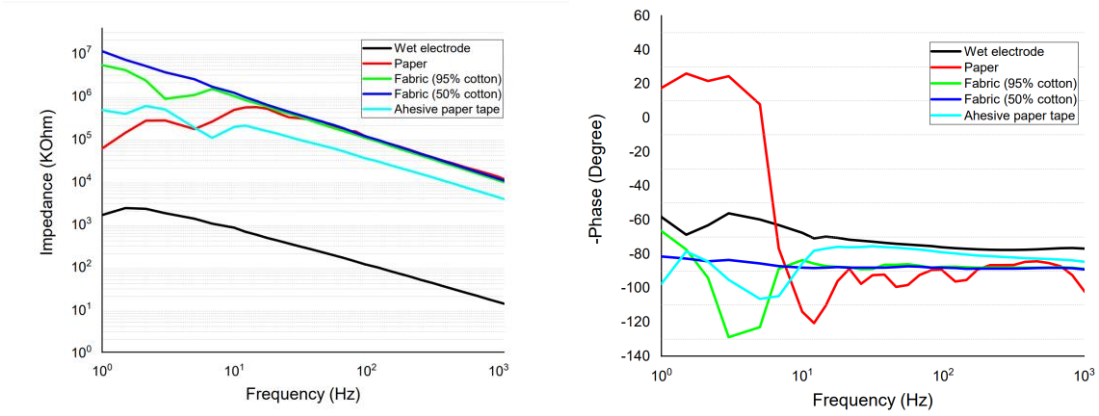

Fig 3.6 Impedance test results

Fig 3.6 shows our results. We test five materials in total, normal adhesive paper tape, A4 paper commonly used by printers, AgCl electrode and two T-shirts of mine, one contains

95% of cotton and 5% of Viscose, which is a manufactured regenerated cellulose fiber, while another shirt contains 50% cotton, 45% viscose and 5% elastane.

AgCl electrodes have the lowest and stable impedance. The impedance is less than 1 MOhms at the range of 10 Hz to 100 Hz. As for the phase plot, the value of AgCl electrodes also keeps stable at low frequency.

3.6.2 Experiments of different thickness insulation layer

We also test the difference between different thickness of insulation layer. We control the thickness through changing the number of pieces of paper. The result is an averaged value from 3 tests. I choose three specific frequency components here, 10 Hz, 50 Hz, and 100 Hz. Since ECG mostly within a range from 0 to 100 Hz, the impedance we test under these three frequency components are more representative. This result is an average of three tests.

Table 1 Impedance of different thickness insulation layer

Layers	10 Hz (MOhms)	50 Hz (MOhms)	100 Hz (MOhms)	Thickness (mm)
1	139.7	34.27	15.76	0.08
2	168.4	61.16	31.35	0.18
3	283.2	76.6	63.49	0.28
4	357.3	100.9	61.5	0.41
5	299.3	108.5	58.35	0.51
6	384.3	102.8	72.1	0.62

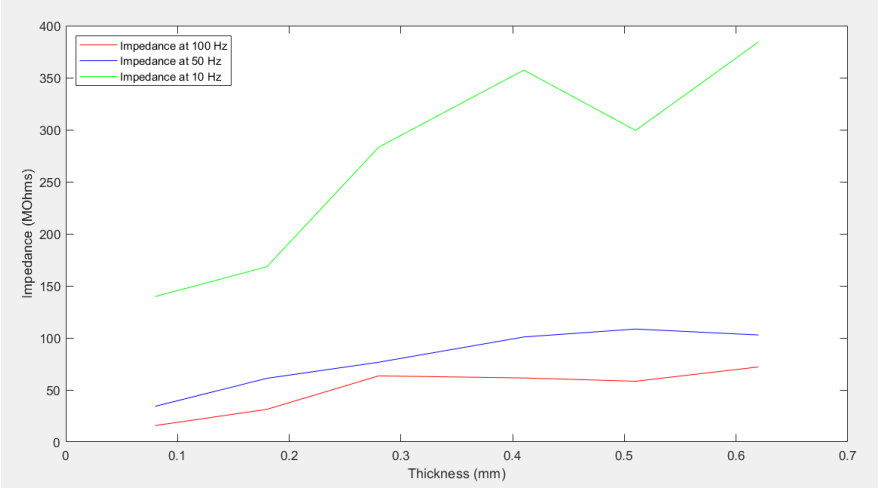

Fig 3.7 Impedance of different thickness insulation layer

From Table 1 and Fig 3.7, we can find that the impedance increases rapidly at low frequency. And the result can't keep stable at low frequency even if this is an averaged value of three tests. We can also get this conclusion from Fig 3.6.

Apart from impedance measurements, we also finish some ECG tests using different thickness paper layers. And this time, we use the results of AgCl electrodes as a gold standard.

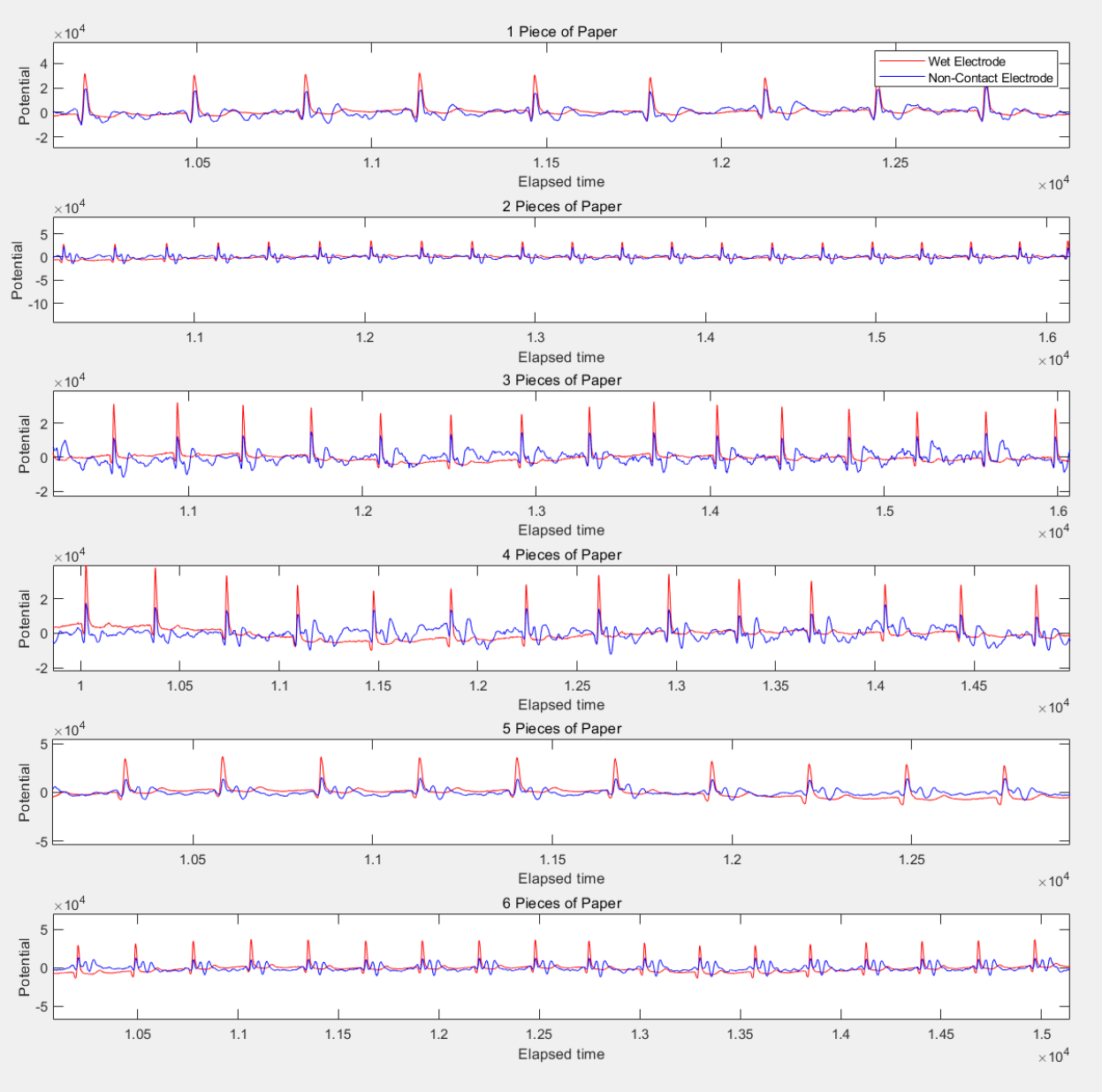

Fig 3.8 ECG tests of different thickness insulation

Table 2 SNR of different thickness insulation

Layers	Test 1 (dB)	Test 2 (dB)	Test 3 (dB)	Average (dB)	Thickness (mm)
1	1.8562	1.1784	0.0257	1.0201	0.08
2	1.5840	0.9593	1.5159	1.3531	0.18
3	1.0897	1.4925	2.2985	1.6269	0.28

4	2.8055	1.2741	2.5227	2.2008	0.41
5	4.1375	4.8455	5.5502	4.8444	0.51
6	6.0142	6.9701	4.2093	5.7312	0.62

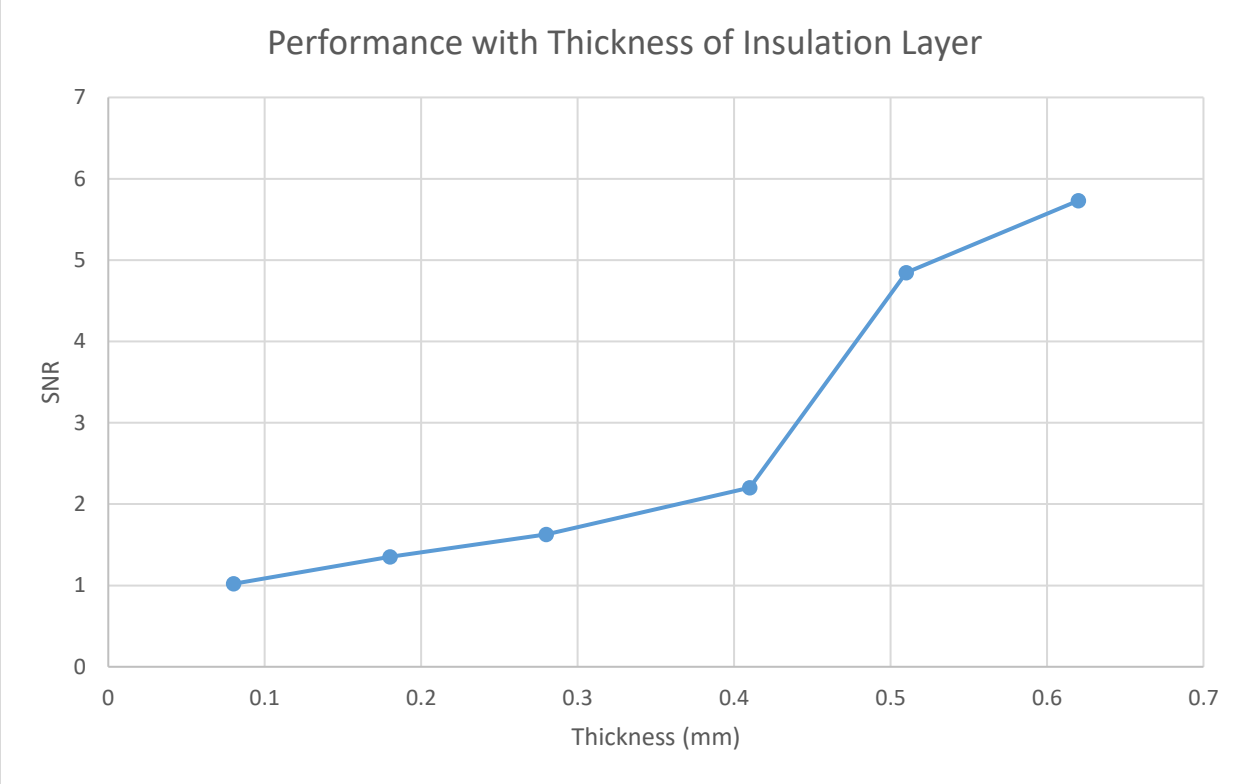

Fig 3.9 SNR of different thickness insulation

Fig 3.9 shows the R peak is very clear when the thickness is less than 0.5 mm. We can still see the peak when the thickness is up to 0.6 mm but there is another pattern or another kind of waveform dominant our signal. Fig 3.10 and table 2 are the quantitative way to prove this conclusion. One possible reason is the motion artifact as this sensor is very sensitive to motion interference. As the increasement of insulation layer thickness, ECG signal is getting weaker and it is much easier to slip between insulation layers, electrodes, and skin.

3.6.3 Experiments with pregnant volunteers

With the approvement of IRB #2020-6342, we complete some measurements with several pregnant volunteers. Here is two of our result.

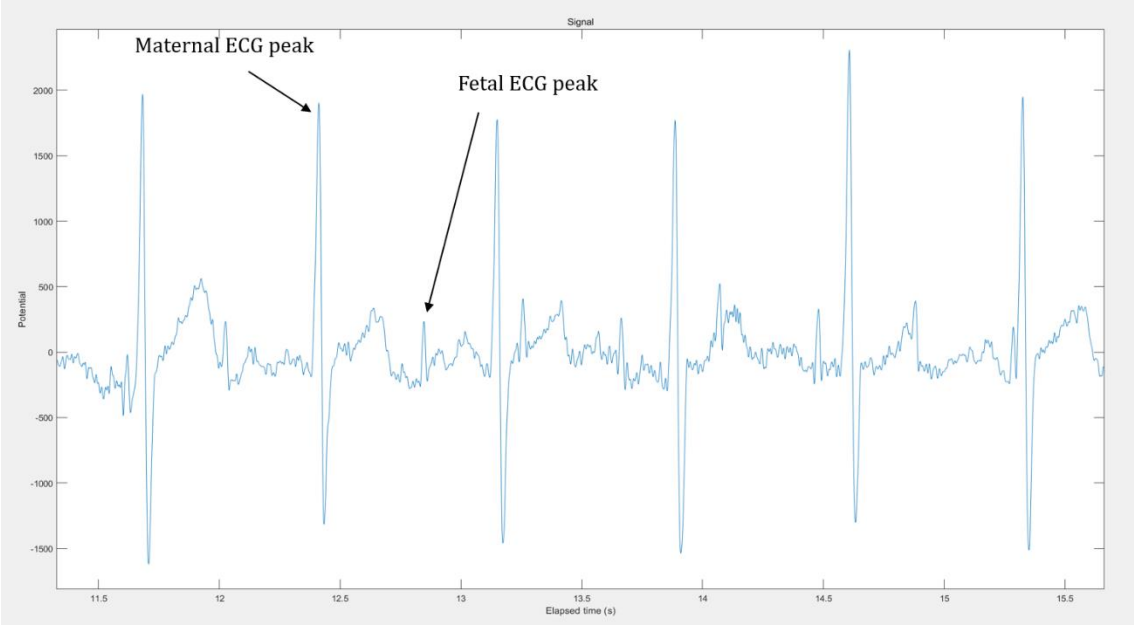

Fig 3.10 Combined fetal and maternal ECG from first volunteer

Fig 3.10 shows the signal from wet electrodes only from first volunteer. We can see both the R peak of maternal ECG and R peak of fetal ECG clearly. The R peak of fetal ECG shows up periodically and stably. But we can't get any useful signal from non-contact electrodes.

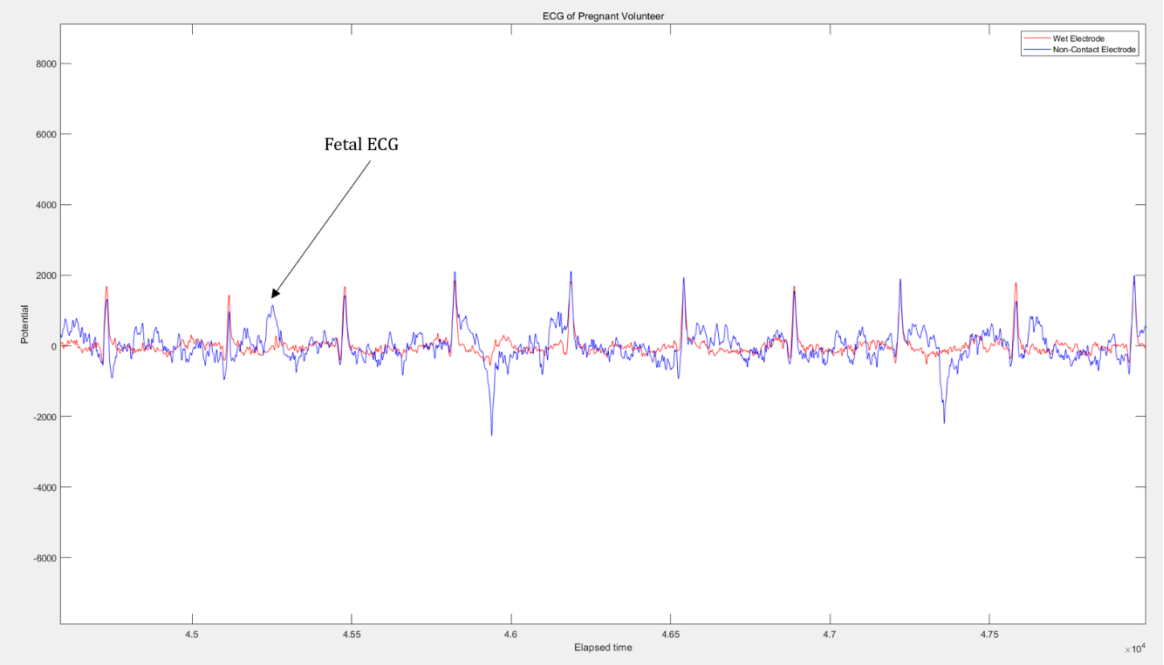

Fig 3.11 Combined fetal and maternal ECG from second volunteer

Fig 3.11 shows the result from the second volunteer. Red plot is the signal from wet electrodes while the blue plot is the signal from non-contact electrodes. We can see the R peak of maternal ECG is very clear. The R peak of fetal ECG is still there but it's not clear compared with the signal from our first volunteer. We did several tests on both volunteers but in each case, the results are similar. The discovery of R peak of both maternal ECG and fetal ECG means we design and fabricate a patch that can measure fetal ECG and maternal ECG successfully. But there are still a lot of questions need to be answered. The signal is not stable and is strongly dependent on different individual test environments, locations and body movement.

Chapter 4

Discussion and Conclusions

In this thesis, we have successfully demonstrated a wireless Bluetooth passive ECG system that can be used to continuously monitor people's abdominal ECG and fetal ECG as well. A lot of experiments are conducted, showing that this sensor patch can obtain very clear, useful and stable ECG from wet electrodes.

As for the non-contact electrodes, we create a non-contact circuits with high sensitivity and validate its basic functionality. We discover the impedance feature of our non-contact electrodes with different insulation materials, different insulation thickness and at different frequency. We also test the ECG signal using different insulation thickness up to 0.6 mm. The minimum SNR is as low as 1.0 dB which is pretty good. When the thickness goes up to 0.5 mm, the signal with the SNR is 5.7 dB becomes a little unstable compared with others. But it is still acceptable and clear.

We also try to complete some measurements with pregnant volunteers. The signal of wet electrodes can be thought as stable and clear. But the fetal signal of non-contact electrodes strongly depends on different individual environments, locations and body movements. We can't guarantee we can get fetal ECG. There are a lot of work to do in the future.

In the next, we will do further work about different materials, different thickness and different electrode area to discover how they will affect impedance and our signals. This sensor is also a proof of a mutual product of fetal maternal ECG. This work will be continued

in our lab. During this pandemic, I believe it will bring some people convenience and safety if it can be on the market.

References

1. Sharma, M., et al., *Cuff-less and continuous blood pressure monitoring: a methodological review*. Technologies, 2017. **5**(2): p. 21.
2. Sholapurkar, S., *The unresolved role of cardiotocography (CTG), fetal ECG (STAN) and intrapartum fetal pulse oximetry (IFPO) as diagnostic methods for fetal hypoxia.* Journal of Obstetrics and Gynaecology, 2014. **34**(8): p. 757-757.
3. Clifford, G.D., et al., *Non-invasive fetal ECG analysis.* Physiological measurement, 2014. **35**(8): p. 1521.
4. Belfort, M.A., et al., *A randomized trial of intrapartum fetal ECG ST-segment analysis.* New England Journal of Medicine, 2015. **373**(7): p. 632-641.
5. Blankertz, B., et al. *A note on brain actuated spelling with the Berlin brain-computer interface*. in *International Conference on Universal Access in Human-Computer Interaction*. 2007. Springer.
6. Prutchi, D. and M. Norris, *Design and development of medical electronic instrumentation: a practical perspective of the design, construction, and test of medical devices*. 2005: John Wiley & Sons.
7. Portelli, A.J. and S.J. Nasuto, *Design and development of non-contact bio-potential electrodes for pervasive health monitoring applications.* Biosensors, 2017. **7**(1): p. 2.
8. Lopez, A. and P.C. Richardson, *Capacitive electrocardiographic and bioelectric electrodes.* IEEE Transactions on Biomedical Engineering, 1969(1): p. 99-99.
9. Guger, C., G. Krausz, and G. Edlinger, *Brain-computer interface control with dry EEG electrodes*. 2011: Citeseer.
10. Bergey, G.E., R.D. Squires, and W.C. Sipple, *Electrocardiogram recording with pasteless electrodes.* IEEE Transactions on Biomedical Engineering, 1971(3): p. 206-211.
11. Lee, K., et al. *Noise reduction for non-contact electrocardiogram measurement in daily life*. in *2009 36th Annual Computers in Cardiology Conference (CinC)*. 2009. IEEE.
12. Harland, C., T. Clark, and R. Prance, *Electric potential probes-new directions in the remote sensing of the human body.* Measurement Science and technology, 2001. **13**(2): p. 163.
13. Searle, A. and L. Kirkup, *A direct comparison of wet, dry and insulating bioelectric recording electrodes.* Physiological measurement, 2000. **21**(2): p. 271.
14. Harland, C., T. Clark, and R. Prance, *Non-Invasive Human Body Electrophysiological Measurements Using Displacement Current Sensors.* Rev. Sci. Instrum, 2002. **11**: p. 291.
15. Sullivan, T.J., S.R. Deiss, and G. Cauwenberghs. *A low-noise, non-contact EEG/ECG sensor*. in *2007 IEEE Biomedical Circuits and Systems Conference*. 2007. IEEE.
16. Oehler, M., et al., *A multichannel portable ECG system with capacitive sensors.* Physiological measurement, 2008. **29**(7): p. 783.
17. Dupre, A., S. Vincent, and P.A. Iaizzo, *Basic ECG theory, recordings, and interpretation,* in *Handbook of cardiac anatomy, physiology, and devices*. 2005, Springer. p. 191-201.
18. Lilly, L.S. and E. Braunwald, *Braunwald's heart disease: a textbook of cardiovascular medicine*. Vol. 2. 2012: Elsevier Health Sciences.
19. Lilly, L.S., *Pathophysiology of heart disease: a collaborative project of medical students and faculty*. 2012: Lippincott Williams & Wilkins.
20. Tereshchenko, L.G. and M.E. Josephson, *Frequency content and characteristics of ventricular conduction.* Journal of electrocardiology, 2015. **48**(6): p. 933-937.

21. Thakor, N.V. and Y.-S. Zhu, *Applications of adaptive filtering to ECG analysis: noise cancellation and arrhythmia detection.* IEEE transactions on biomedical engineering, 1991. **38**(8): p. 785-794.
22. Chi, Y.M., *Non-contact biopotential sensing*. 2011, UC San Diego.
23. Le, T., et al. *Unobtrusive continuous monitoring of fetal cardiac electrophysiology in the home setting*. in *2018 IEEE SENSORS*. 2018. IEEE.